Nanoscale

PAPER

View Article Online
View Journal | View Issue

Cite this: *Nanoscale*, 2014, **6**, 11246

Bias induced transition from an ohmic to a non-ohmic interface in supramolecular tunneling junctions with Ga_2O_3/EGaIn top electrodes†

Kim S. Wimbush,[a] Raluca M. Fratila,[a] Dandan Wang,[b] Dongchen Qi,‡[c] Cao Liang,[b] Li Yuan,[b] Nikolai Yakovlev,[c] Kian Ping Loh,[be] David N. Reinhoudt,[a] Aldrik H. Velders*[ad] and Christian A. Nijhuis*[bce]

Received 28th May 2014
Accepted 16th July 2014

DOI: 10.1039/c4nr02933j

www.rsc.org/nanoscale

This study describes that the current rectification ratio, $R \equiv |J|(-2.0\ \text{V})/|J|(+2.0\ \text{V})$ for supramolecular tunneling junctions with a top-electrode of eutectic gallium indium (EGaIn) that contains a conductive thin (0.7 nm) supporting outer oxide layer (Ga_2O_3), increases by up to four orders of magnitude under an applied bias of >+1.0 V up to +2.5 V; these junctions did not change their electrical characteristics when biased in the voltage range of ±1.0 V. The increase in R is caused by the presence of water and ions in the supramolecular assemblies which react with the Ga_2O_3/EGaIn layer and increase the thickness of the Ga_2O_3 layer. This increase in the oxide thickness from 0.7 nm to ~2.0 nm changed the nature of the monolayer–top-electrode contact from an ohmic to a non-ohmic contact. These results unambiguously expose the experimental conditions that allow for a safe bias window of ±1.0 V (the range of biases studies of charge transport using this technique are normally conducted) to investigate molecular effects in molecular electronic junctions with Ga_2O_3/EGaIn top-electrodes where electrochemical reactions are not significant. Our findings also show that the interpretation of data in studies involving applied biases of >1.0 V may be complicated by electrochemical side reactions which can be recognized by changes of the electrical characteristics as a function voltage cycling or in current retention experiments.

Introduction

The mechanisms of charge transport across organic electronic devices are important to understand in applications ranging from photovoltaics,[1] organic light emitting diodes,[2] flexible electronics,[3] molecular electronics,[4,5] to organic electronics.[6–8] In general, the organic-metal, *e.g.*, thiol–Au, and semiconductor–metal interfaces, *e.g.*, Al_2O_3/Al, play a key role in the electrical properties and performance of these devices.[9–11] In molecular electronics the nature of the metal–molecule interfaces has been of major concern,[4,5,10,12–26] but difficult to address experimentally directly.[25,27,28] It determines how molecular orbitals couple to the electrodes electronically,[14,15,26] the value of the contact resistance,[14,18–21,23,24] and the electronic function of the device. In addition, the nature of the contact may also determine whether the current *vs.* voltage characteristics are ohmic or non-ohmic.[29] Especially the presence of (thin) layers of metal oxides in tunneling junctions is of concern and complicates the interpretation of data from junctions prepared with oxidizable electrodes.[2,30–36]

Every molecular electronic device is a physical-organic system with its unique electronic, chemical, and supramolecular structure consisting of at least two electrodes, the organic part, and two interfaces between the electrodes and the organic part.[37] An "ideal" technique to investigate the contribution of each of the components of the junctions to the electrical characteristics is still not available.[27,38–41] At best, the electronic properties of the junctions can be investigated as a function of one component while minimizing the potential changes to the other components.

Although there is no "ideal" technique to form electrical contacts to self-assembled monolayers (SAMs), methods have

[a]*Laboratory of Supramolecular Chemistry and Technology, MESA + Research Institute, University of Twente, 7500 AE Enschede, The Netherlands. E-mail: aldrik.velders@wur.nl; Tel: +31317485970*

[b]*Department of Chemistry, National University of Singapore, 3 Science Drive 3, Singapore 117543, Singapore. E-mail: christian.nijhuis@nus.edu.sg; Tel: +65 6516 2667*

[c]*Institute of Materials Research and Engineering, A*Star, 3 Research Link, Singapore, 117602, Singapore*

[d]*Laboratory of BioNanoTechnology, Wageningen University, PO Box 8038, 6700 EK Wageningen, The Netherlands*

[e]*Graphene Research Centre, National University of Singapore, 6 Science Drive 2, Singapore 117546, Singapore*

† Electronic supplementary information (ESI) available: Nomenclature, synthesis of compounds, preparation of supramolecular tunneling junctions, $J(V)$ measurements of tunneling junctions, $J(V)$ characteristics of oxidized Ga_2O_3/EGaIn tips, Kelvin probe measurements, photoelectron spectroscopy and ellipsometry measurements. See DOI: 10.1039/c4nr02933j

‡ Current address: Department of Physics, La Trobe University, Bundoora, Victoria 3086, Australia

been developed to avoid direct metal evaporation on SAMs. The latter gives rise to junctions that are prone to defects, such as metal filaments,[42,43] or chemical changes to the SAM.[44,45] Moreover, this gives a high percentage of short circuits (ohmic behavior).[46–48] Alternative fabrication methods use liquid metal electrodes,[49–52] protection layers such as graphene (derivatives),[3,53–55] or conducting polymers,[51,56,57] to protect the SAM against potential damage during the metal deposition step.

To avoid the problems associated with direct evaporation of metals on the SAM, we use a non-Newtonian liquid-metal top-electrode of a eutectic mixture of Ga and In (EGaIn; see below) that forms electrical contacts to SAMs in a non-invasive manner.[58] This technique has three properties that make it an attractive platform to perform physical-organic studies of charge transport across SAMs. (i) It yields SAM-based junctions that are stable enough to withstand more than 100 $J(V)$ scans in the bias range of $\pm$1.0 V for long enough periods of time (up to 16 h), and allows to collect statistically large numbers of data (N > 400) and produces high yields of working junctions (80–100%).[59,60] (ii) It is sensitive enough to perform detailed physical-organic studies of charge transport across SAMs as a function of the chemical and supramolecular structure of the SAMs.[22,34,35,37,58,60–70] (iii) It avoids the use of photolithography or clean room conditions and is straightforward to setup in an ordinary lab. The EGaIn-technique has also disadvantages: it lacks the stability required for commercial applications and the thin layer of Ga_2O_3 of 0.7 nm adds complexity for the interpretation of the data. We believe that this thin layer of gallium oxide forms an ohmic contact with the SAMs (but with a yet unknown contact resistance) and as such can function as a non-invasive electrode-interface contact. The Ga_2O_3 layer is highly conductive (3.3×10^{-4} Ω cm^2),[70] and is highly defective and contains oxygen vacancies and indium oxides.[71] Also it adds mechanical stability to the junctions and prevents the bulk EGaIn from alloying with the bottom-electrode material. Detailed investigations of charge transport using EGaIn on various kinds of SAMs include *n*-alkanethiolates,[58,63,66,70] conjugated molecules,[61,62,68] ferrocene (Fc) functionalized *n*-alkanethiolates,[34,35,37,64,65] and supramolecular assemblies.[67] These studies have led to the conclusion that the electrical properties of these junctions are dominated by the chemical and supramolecular structure of the SAMs, and not by the thin conductive layer of 0.7 nm of predominantly Ga_2O_3 on the top-electrode.[22,34,35,37,58,60–70]

This paper describes tunneling junctions with the Ga_2O_3/EGaIn top-electrode in contact with a SAM of well-defined hexagonally packed heptathioether-functionalized β-cyclodextrins (βCD) on template-stripped gold (Au^{TS}) onto which a monolayer of dendrimers can be adsorbed (Fig. 1).[72–76] These supramolecular SAMs are relatively thick (~3 nm), and therefore the junctions that incorporated them withstand large applied biases; the junctions were stable against voltage cycling in the relatively large bias range of $\pm$2.0 V for 100 cycles (one cycle = 0 V $\rightarrow$ 2.0 V $\rightarrow$ 0 V $\rightarrow$ $-$2.0 V $\rightarrow$ 0 V; each cycle took about 80 s to complete), and voltage pulses (V_{pulse}) stepped from 0 V up to +2.5 V for a period of up to one hour after which the voltage was stepped back to 0 V. Remarkably, the junctions described in this paper changed their electrical characteristics when the Ga_2O_3/EGaIn top-electrode was biased positively with a bias of >+1.0 V, regardless of the supramolecular structure of the SAM, with an increase in rectification ratio ($R \equiv |J|(-2.0\,V)/|J|(+2.0\,V)$, where J = current density) of up to four orders of magnitude. The SAM–top electrode interface was found to change from an ohmic to a non-ohmic contact, which, in turn, dominated the charge transport characteristics and we believe it was the origin of the observed increase in R. We note that non-ohmic contacts do not necessarily result in rectifying junctions, but we prefer to use this term as we do not know the exact nature of the SAM//top-electrode contact when the junctions rectify (see below). The change from an ohmic to a non-ohmic contact is attributed to the *in situ* formation of a thick layer of gallium oxides (~2 nm) under applied bias due to the presence of water and ions, *i.e.*, H_3O^+, protonated amines and Cl^-, in the supramolecular SAM. These findings are also supported by the work of Dickey and co-workers[77,78] who reported that thick layers of gallium oxides can grow on EGaIn in acidic aqueous media.

The results described in this paper corroborate previous reports[23,30,34,36,53,79] that the interpretation of data generated by molecular junctions should be performed with attention to constraints, and the voltage window in which the Ga_2O_3/EGaIn electrode can be used without concerns for modifying its properties. Our data, on the one hand, clearly demonstrate the practical usefulness of the "EGaIn technique" to conduct studies of charge transport across SAM-based junctions. On the other hand, studies focused on charge transfer characteristics involving supramolecular structures that contain chemisorbed water and ions should be limited to an applied DC bias of maximum +1.0 V to avoid oxidation of the top-electrode which is close to the break down field of approximately 0.8 GV m^{-1} for junctions with SAMs of *n*-alkanethiolates.[65,80] For SAMs that do not contain chemisorbed water, and/or ions, bias-induced changes of the electrical characteristics of the junctions have not been observed (but these studies also did not involve bias ranges larger than $\pm$1.0 V).[22,34,35,37,58,60–70] It is likely that bias-induced oxidation of the top-electrode with water from ambient air will require much larger biases (see below) than +1.0 V to induce anodic growth of the Ga_2O_3 layer at a rate relevant to the experimental time scales. Studies of charge transport using DC experiments involving bias ranges equal to or smaller than +1.0 V are not dominated by a non-ohmic contact; the thin gallium oxide layer of 0.7 nm acts as an ohmic contact (and does not influence R) and allows the molecular/supramolecular structure to dominate the junctions' charge transport characteristics.

Results and discussion

The following sections describe the chemical structures of the supramolecular tunneling junctions, the $J(V)$ characteristics of the junctions as a function of the number of voltage cycles (with one voltage cycle defined as a sweep from 0 V $\rightarrow$ 2.0 V $\rightarrow$ 0 V $\rightarrow$ $-$2.0 V $\rightarrow$ 0 V which was completed in about 80 s), and the $J(V)$ characteristics as a function of the duration and height of the

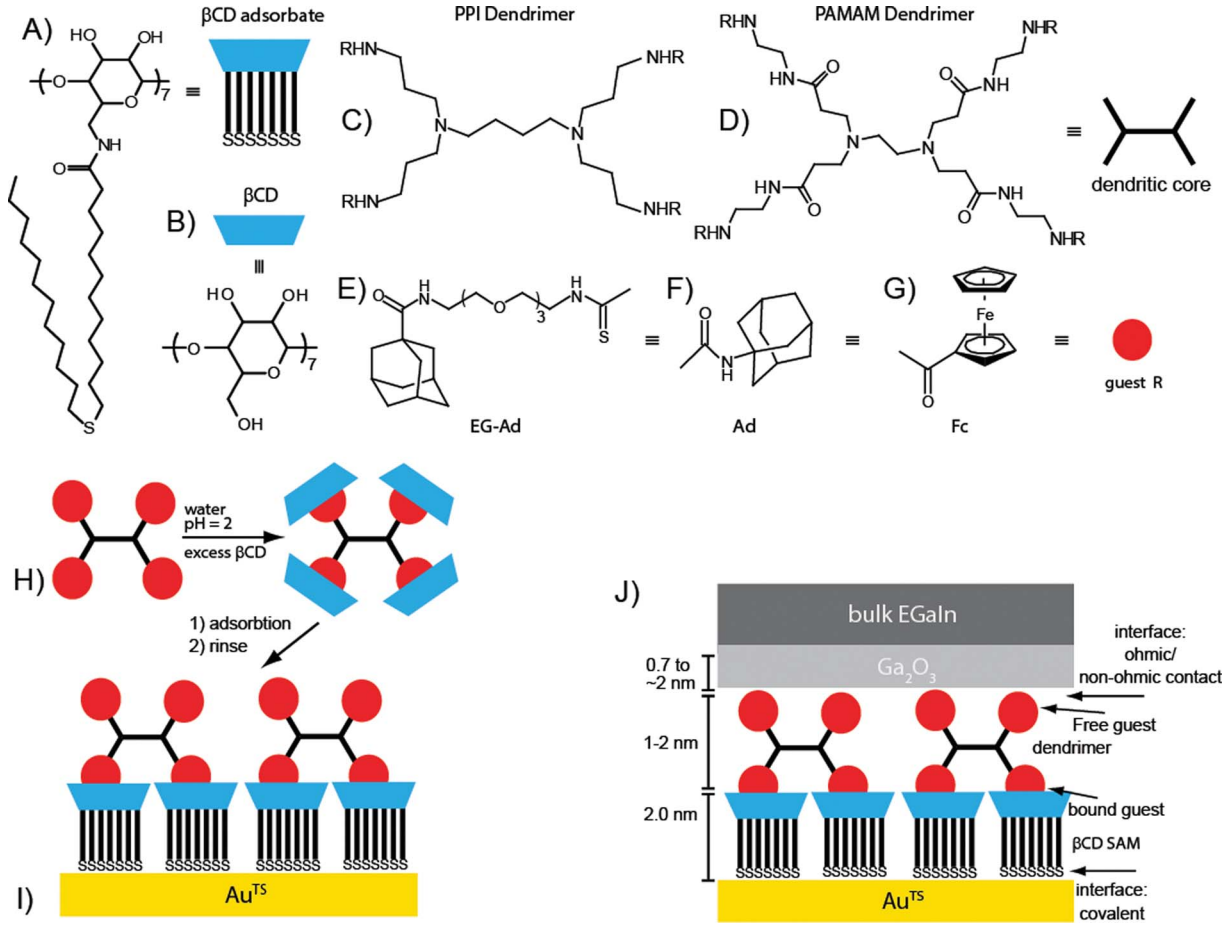

Fig. 1 (A–G) The molecular structures of the components used to assemble the supramolecular junctions: the heptathioether-functionalized β-cyclodextrin adsorbate (A) to form the βCD SAM, or host surface, the native β-cyclodextrin (B), the dendritic core of the poly(propylene) imine (PPI; C), poly(amido amine) (PAMAM); D) dendrimer functionalized with an adamantyl (Ad) with a tetra-ethylene glycol (EG) tether (E), Ad (F), or ferrocene (Fc) (G). (H–J) Schematic illustration of the assembly of the supramolecular junctions. The dendrimers were dissolved in an aqueous solution by complexation of the guest end group moieties to native βCD at pH = 2 to ensure protonation of the core amines and to force the dendrimers to adopt a fully extended conformation (H). The dendrimers were adsorbed on a pre-formed host-surface by simply immersing the host surface into the aqueous solutions of the dendrimers (I). The surfaces were rinsed with water to remove physisorbed dendrimers and native βCD. The Ga_2O_3/EGaIn top-electrode was formed on the supramolecular assembly (J). By varying the core type and terminal functionality, we controlled the packing density, and the number of interactions of the dendrimers with the host surface. We formed junctions with four different types of dendrimers, *i.e.*, G1-PPI–$(Ad)_4$, G1-PPI–$(Fc)_4$, G0-PAMAM–$(Ad)_4$, and G0-PAMAM–$(EG\text{-}Ad)_4$, and with the bare βCD SAM to control the number of interactions of the dendrimer guest molecules with the host surface. Here an example is given for a dendrimer with two moieties interacting with the host surface and two free moieties (see Table 1 for the numbers of interacting and free moieties for all dendrimers).

voltage pulses (V_{pulse}; for one V_{pulse} the applied bias was stepped from 0 V to the desired applied voltage, and after a predefined period of time t (up to 3600 s) the bias was stepped back to 0 V). We finally discuss the dependence of the increase of R on the molecular structure of the SAM and on the chemical structure of the bottom and top electrodes.

Supramolecular tunneling junctions

Fig. 1 shows the supramolecular platform and junction schematically. We have adsorbed four different guest molecules on a well-defined hexagonally packed SAM of host molecules of heptathioether-functionalized βCD on Au^{TS} ("the molecular printboard" Fig. 1A): generation-1 poly(propylene) imine dendrimers (Fig. 1C) with four adamantyl (Fig. 1F) units (G1-PPI–$(Ad)_4$), or four ferrocene (Fig. 1G) units (G1-PPI–$(Fc)_4$), and a generation-0 poly(amido amine) dendrimer (Fig. 1D) with four adamantyl units (G0-PAMAM–$(Ad)_4$), or with a tetra-ethylene glycol tether (Fig. 1E) separating the Ad from the dendritic core (G0-PAMAM–$(EG\text{-}Ad)_4$).[72–74,76] We chose to use both Fc and Ad terminated dendrimers because in previous studies we were able to control the rectification in supramolecular junctions as a function of molecular structure, with Fc terminated dendrimers rectifying the current whilst Ad terminated dendrimers did not.[67]

Fig. 1H–J show schematic illustrations of the immobilization of the dendrimers on the host-surface and the supramolecular tunneling junctions. To adsorb the dendrimers on the molecular printboard, the dendrimers were dissolved in water by protonation of the core amines with aqueous HCl to force the

dendrimers to adopt fully extended conformations for complexation of the Ad or Fc termini (Fig. 1H) to native βCD (Fig. 1B).[74,76,81] In a second step, the dendrimers were adsorbed on a pre-formed βCD Au surface to which the Fc and Ad moieties can bind (Fig. 1I). The major driving force for the adsorption of the dendrimers is the 100 times higher effective concentration of βCD hosts on the surface than in solution.[82,83] The dendrimers form stable assemblies on the host surface because of the multiple host–guest interactions.[75,76] The number of interactions of the dendrimer with the βCD host surface depends on the distance of the terminal functional moieties from one another. This can be controlled by using dendrimers with different distances between the core and terminal functional group, *i.e.*, PPI (Fig. 1C) or PAMAM (Fig. 1D), or by simply introducing tethers of ethylene glycol (Fig. 1E). The dendrimers used in this study have two, three, or four Fc– or Ad–βCD interactions with the printboard (see Table 1).[74,76] The surface coverage of the dendrimers depends on the number of host–guest interactions that the dendrimers can have with the βCD SAMs. Only dendrimers with three or four interactions form monolayers with (nearly) 100% surface coverage (Table 1).[74,76,82] Thus, the dendrimer–βCD supramolecular assemblies anchored on Au^{TS} surfaces contain water and ions (*i.e.*, H_3O^+, protonated amines and Cl^- counter-ions). We formed electrical contact with the supramolecular βCD–dendrimer assemblies using Ga_2O_3/EGaIn as the top-electrode material following procedures previously reported (Fig. 1J).[67]

The effects of voltage cycling and voltage pulses

Fig. 2 shows the change of the $J(V)$ characteristics of a junction of Au^{TS}–βCDSAM//G1-PPI–$(Fc)_4$//Ga_2O_3/EGaIn as a function of voltage cycling ($N = 100$) in the range over ±2.0 V (Fig. 2A), and the values of J measured at +2.0 V and −2.0 V (Fig. 2C), and R, as a function of N (Fig. 2E). The junctions clearly changed their electrical characteristics as a function of N. The currents at a negative bias increased by about one order of magnitude, while the currents at a positive bias decreased by one order of magnitude (indicated by the red arrows), resulting in a large increase of the rectification ratio from 1.2 (at $N = 1$) to 2.4×10^2 (at $N = 100$). Fig. S2† shows similar results for junctions with the βCD SAM and with the G1-PPI–$(Ad)_4$ dendrimer adsorbed on a βCD SAM. Thus, subjecting these junctions with supramolecular assemblies to a large number of scans at relatively large applied voltages changed the electrical properties of the junctions.

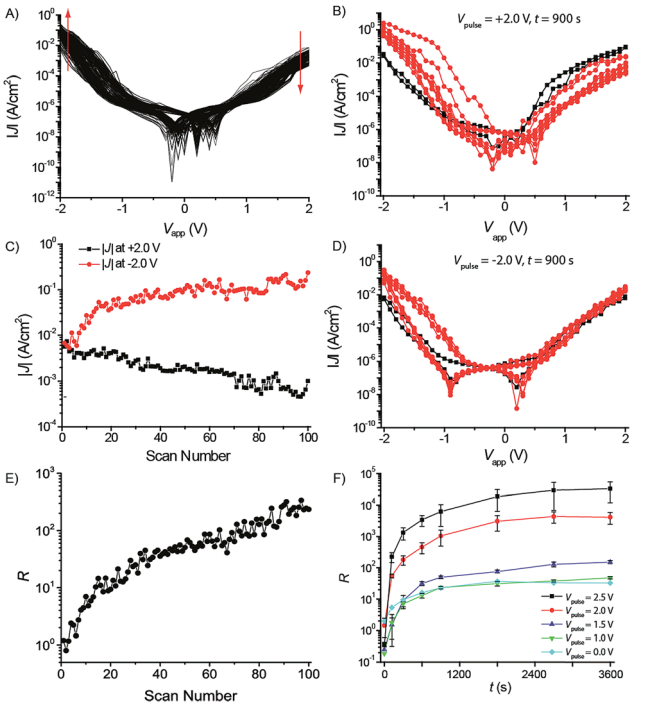

Fig. 2 The electrical characteristics of Au^{TS}–βCDSAM//G1-PPI–$(Fc)_4$//Ga_2O_3/EGaIn junctions. (A) Semi-log plot of 100 $|J|(V)$ scans measured over an applied voltage range of ±2.0 V; (C) semi-log plot of the value of $|J|$ measured at −2.0 V and +2.0 V *vs.* number of scans, and (E) the value of R as a function number of scans. (B and D) Semi-log plot of a $|J|(V)$ scan recorded on the Au^{TS}–βCDSAM//G1-PPI–$(Fc)_4$//Ga_2O_3/EGaIn junction before and 5 scans after $V_{pulse} = +2.0$ V (B), and $V_{pulse} = -2.0$ V (D). (F) Semi-log plot of the value of R of junctions of Au^{TS}–βCDSAM//G1-PPI–$(Fc)_4$//Ga_2O_3/EGaIn as a function voltage pulse of +1.0 V (▼), +1.5 V (▲), +2.0 V (●), +2.5 V (■) measured by performing five $J(V)$ scans ±2.0 V at $t = 120$, 300, 600, 900, 1800, 2700, and 3600 s. To account for the increase of the value of R while performing the five $J(V)$ scans, the plot also includes the values of R as a function of scan number, or without voltage pulse across the junction (♦, and indicated by '0 V').

Table 1 The number of interactions and surface coverages of the dendrimers on the βCD SAM and the rectification ratios before and after a voltage pulse (V_{pulse})

Junction[a]	Number of interactions[b]	Number of free moieties[c]	Surface coverage[d] (%)	R before[e] V_{pulse}	R after[f] V_{pulse}
PPI–Fc	2	2	89	0.35	3.3×10^4
PPI–Ad	2	2	>95	0.10	2.9×10^3
PAMAM–Ad	3	1	~100	1.1	2.6×10^2
PAMAM–EG-Ad	4	0	~100	1.8	4.2×10^2
βCD SAM	—	—	—	0.19	2.5×10^5

[a] PPI–Fc = Au^{TS}–βCDSAM//G1-PPI–$(Fc)_4$//Ga_2O_3/EGaIn; PPI–Ad = Au^{TS}–βCDSAM//G1-PPI–$(Ad)_4$//Ga_2O_3/EGaIn; PAMAM–Ad = Au^{TS}–βCDSAM//G1-PAMAM–$(Ad)_4$//Ga_2O_3/EGaIn; PAMAM–EG-Ad = Au^{TS}-βCDSAM//G1-PPI–$(EG\text{-}Ad)_4$//Ga_2O_3/EGaIn; and βCD SAM = Au^{TS}–βCDSAM//Ga_2O_3/EGaIn. [b] The number of Fc or Ad moieties that form host–guest interactions with the βCD SAM (out of four). [c] The number of unbound Fc or Ad moieties. [d] Surface coverage (%) of the dendrimer adsorbed to the supramolecular platform taken from ref. 74 and 76. [e] The value of R measured at ±2.0 V at the start of the experiment. [f] The value of R measured at ±2.0 V after $V_{pulse} = +2.5$ V of $t = 3600$ s.

Fig. 2B shows the $J(V)$ characteristics of a junction of Au^{TS}–βCDSAM//G1-PPI–$(Fc)_4$//Ga_2O_3/EGaIn before (■) and after (●) applying a voltage pulse (V_{pulse} (V)) of +2.0 V for $t = 900$ s. The rectification ratio increased from 0.3 (measured prior V_{pulse}, or at $t = 0$ s) to 1.1×10^2. In contrast, a modest change in the rectification ratio was observed from 0.8 to 9.4 when a voltage pulse at the opposite bias ($V_{pulse} = -2.0$ V for $t = 900$ s) was applied (Fig. 2D). The changes in the values of R as a result of these voltage pulses were recorded as $J(V)$ curves before and after each V_{pulse} in the bias range of ±2.0 V. We recorded five $J(V)$ traces to determine the changes in R, in order to minimize the impact of these (R-determining) scans on R (*vide supra*, see Fig 2A, C and E). The modest change observed in R when applying $V_{pulse} = -2.0$ V is likely due to the five $J(V)$ scans ±2.0 V rather than due to the voltage pulse itself (see below and Fig. 2F).

These supramolecular junctions can be subjected to biases of up to ~±2.5 V under DC conditions. Hence, we studied the changes in the electrical characteristics as a function of V_{pulses} of +1.0, +1.5, +2.0, and +2.5 V over time intervals, t (s), of $t = 120$, 300, 600, 900, 1800, 2700, and 3600 s. Fig. 2F also shows the effect of the voltage cycling on the value of R (indicated as $V_{pulse} = 0$ V) to discriminate between the changes of R due to voltage cycling and V_{pulse}. The rectification ratio increases as a function of V_{pulse} and t. The largest increase in the rectification ratio from 0.35 (at $t = 0$ s) to 3.3×10^4 was observed for a V_{pulse} of +2.5 V for 3600 s. It seems that after 1800 s the maximum value of R had been reached at a given value of V_{pulse}. These measurements were performed at least in duplicate to demonstrate their reproducibility (Fig. S3A†). In some of the duplicate measurements there was a sharp uncharacteristic decrease in R with an increase in t, *i.e.*, in Fig. S3A† for $V_{pulse} = 2.0$ V (2) at $t = 45$ min. This is likely due to a small drift in the Ga_2O_3/EGaIn tip during the two hour measuring period. This drift renders other areas of the Ga_2O_3/EGaIn tip that are less oxidized, with a thinner Ga_2O_3 layer, in contact with the SAM, which decreases R.

The value of R seems to increase exponentially as a function of V_{pulse} (Fig. S3F†) and, currently, we do not know the details of this dependence of the increase of R as a function of V_{pulse}. However, we note that the increase of the value of R, due to V_{pulse} at +1.0 V and at $t = 3600$, is very similar to changes in the value of R resulting from five voltage cycles of ±2.0 V, *i.e.*, without applying a V_{pulse} (Fig. 2F). Thus, a V_{pulse} of +1.0 V has no effect on the values of R (as expected considering the exponential dependence of the value of R on V_{pulse}; see Fig. S3F†). This means that R is dominated by the molecular properties of the supramolecular junctions and does not change its electrical characteristics at applied biases of ≤+1.0 V.

The dependence of the increase of R on the molecular structure

As described above, we observed an increase of R when performing extensive voltage cycling with relatively large voltage windows. In previous studies,[67] we attributed the rectification with values of R of up to two orders of magnitude observed in the supramolecular junctions of Au^{TS}–βCDSAM//G1-PPI–$(Fc)_4$//Ga_2O_3/EGaIn and Au^{TS}–βCDSAM//G1-PPI–$(Fc_2)_4$ to molecular effects involving the Fc functional groups of the dendrimer. The Fc groups have energetically accessible HOMO levels, *i.e.*, close in energy to the Fermi-levels of the electrodes, and positioned asymmetrically inside the junction in close proximity to the Ga_2O_3/EGaIn top electrode. In that particular study, 20 sweeps were taken to calculate R and we could relate the observed R to molecular effects based on the reference experiments with adamantane instead of ferrocene functionalized dendrimers. In a separate study, SAMs of more simple chemical structures, *i.e.*, $SC_{11}Fc$ and $SC_{11}Fc_2$ (which do not contain chemisorbed water or ions),[22,34,37,64] also rectified currents with values of R of two orders of magnitude and did not change their $J(V)$ characteristics as a result of voltage cycling over the range of ±1.0 V for 100 times.[34] The now presented large increase in the values of R of three to four orders of magnitude for the supramolecular junctions induced by applying a V_{pulse} of >+1.0 V for 1 h is therefore likely not a molecular property of the junctions.

We hypothesize that the increase in the values of R in Au^{TS}–βCDSAM//G1-PPI–$(Fc)_4$//Ga_2O_3/EGaIn originates from changes in the chemical composition of the tunneling junctions. These involve the heptathioether βCD SAM on the Au surface, the Au^{TS} bottom-electrode, or the Ga_2O_3/EGaIn top-electrode, which in turn will also change the nature of the interfaces of the electrodes with the monolayers. To determine if the large increase in the value of R as a result of V_{pulse} is molecular in origin, we studied the electrical properties of junctions in which the Fc moieties were replaced by Ad, *i.e.*, Au^{TS}–βCDSAM//G1-PPI–$(Ad)_4$//Ga_2O_3/EGaIn and junctions that lack the dendrimer *i.e.*, Au^{TS}–βCDSAM//Ga_2O_3/EGaIn.[67] The adamantane units are not providing HOMO levels close in energy to the Fermi levels of the electrodes and the corresponding two junctions did not rectify current in our previous studies, giving values of R of 0.7 ($\sigma_{log} = 2.5$) and 1.0 ($\sigma_{log} = 3.0$), respectively, when performing 20 scans ±2.0 V.[67] Fig. 3A shows that the values of R of these three different supramolecular junctions increased as a function of the time of V_{pulse} of +2.5 V.

We consecutively investigated the effect of the dendritic core, the number of interactions of the dendrimers with the host surface, and the difference of surface coverages of the dendrimers on the host surface on the changes of the electrical characteristics of the junctions during the experiments described above. We replaced the PPI core by a PAMAM core, *i.e.*, Au^{TS}–βCDSAM//G0-PAMAM–$(Ad)_4$//Ga_2O_3/EGaIn junctions, and formed junctions with tetra-ethylene glycol tethers between the adamantyl groups and the dendritic core, *i.e.*, Au^{TS}–βCDSAM//G0-PAMAM–$(EG\text{-}Ad)_4$//Ga_2O_3/EGaIn junctions (Fig. 1 and S4†). The G0-PAMAM–$(EG\text{-}Ad)_4$ dendrimer binds to the supramolecular platform with all four Ad units and has no free terminal moieties available to form a contact with the top-electrode. Instead the contact is probably formed by the core/backbone of the dendrimer (Fig. S4E†). The G1-PPI–$(Ad)_4$ dendrimer binds to the supramolecular platform with two (out of four Ad units) and has two free terminal moieties available to form a contact with the top-electrode (Fig. 1). The dendrimers that bind to the host surface with at least three out of four guest moieties form more densely packed monolayers than those dendrimers with only two interacting moieties (Table 1).[74,76,82]

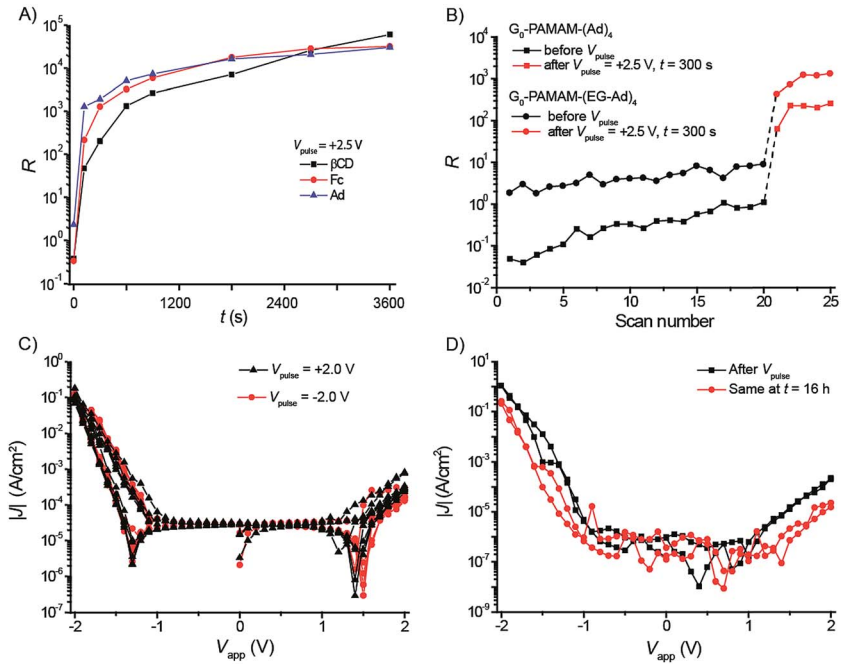

Fig. 3 (A) Semi-log plot of the values of R of junctions of Au^{TS}–βCDSAM//G1-PPI–$(Fc)_4$//Ga_2O_3/EGaIn (●), Au^{TS}–βCDSAM//G1-PPI–$(Ad)_4$//Ga_2O_3/EGaIn (▲), and Au^{TS}–βCDSAM//Ga_2O_3/EGaIn (■), as a function of V_{pulse} = +2.5 V followed by measuring five $J(V)$ traces at t = 120, 300, 600, 900, 1800, 2700, and 3600 s. (B) The values of R as a function of scan number for Au^{TS}–βCDSAM//G0-PAMAM–$(Ad)_4$//Ga_2O_3/EGaIn and Au^{TS}–βCDSAM//G0-PAMAM–(EG-$Ad)_4$//Ga_2O_3/EGaIn junctions subjected to V_{pulse} = +2.5 with t = 300 s between scan numbers 20 and 21. (C) Semi-log plot of five $|J|$(V) curves recorded using a Au^{TS}–βCDSAM//G1-PPI–$(Fc)_4$//Ga_2O_3/EGaIn junction after two voltage pulses (first V_{pulse} = +2.0 V with t = 600 s followed by an additional V_{pulse} = −2.0 V with t = 1200 s). (D) The J(V) curves of Au^{TS}–βCDSAM//G1-PPI–$(Fc)_4$//Ga_2O_3/EGaIn recorded directly after a voltage pulse of +2.5 V with t = 3600 s (■) and 16 h later (●).

Fig. 3B shows the R values of the junctions with the PAMAM dendrimers measured before and after V_{pulse} = +2.5 V with t = 300 s (see Fig. S4F and G† for the $J(V)$ curves). As expected, the value of R increased modestly for both types of junctions during the first 20 scans ±2.0 V. In contrast, for both types of junctions the value of R increased by more than one order of magnitude due to V_{pulse} = +2.5 V. These results indicate that the increase of the value of R is independent of the chemical and supramolecular structure of the SAMs in the tunneling junctions.

We further tested if the changes in the $J(V)$ characteristics are irreversible and stable. The Au^{TS}–βCDSAM//G1-PPI–$(Fc)_4$//Ga_2O_3/EGaIn junction was subjected to a V_{pulse} with the top-electrode biased at −2.0 V for 1200 s, after it had already been subjected to V_{pulse} = +2.0 V for t = 600 s previously (Fig. 3C). In a second experiment, we measured the $J(V)$ characteristics of one junction directly after V_{pulse} = +2.5 V for t = 3600 s and again 16 hours later (Fig. 3D). Both experiments showed that the junctions did not change their $J(V)$ characteristics by applying negative bias or upon aging. We concluded that the changes induced by a large positive bias are stable (over a period of time of at least 16 h) and irreversible (over at least the experimental time scales and bias ranges used here).

Dependence of R on the chemical structure of the electrodes: the bottom-electrode

To determine if the chemical composition of the βCD SAM or if the Au–molecule interface changed during the experiments, we examined the SAMs on Au^{TS} before and after they had been subjected to V_{pulse} = +2.5 V for t = 900 s by X-ray photoelectron spectroscopy (XPS). We used the flexibility of our approach to contact SAMs electrically which makes it possible to assemble a junction, lowering the cone-shaped Ga_2O_3/EGaIn top-electrode using the micromanipulator (see Experimental). After performing the measurements, the junction was disassembled by lifting up the cone-shaped Ga_2O_3/EGaIn top-electrode using the same micromanipulator. This exposes the SAM that had originally been embedded in the Au^{TS}–βCDSAM//Ga_2O_3/EGaIn structure. The XPS measurements were carried out on areas of the sample where the βCD SAM had been biased, and were compared to the areas on the sample that had not been biased. Fig. 4 shows the XPS maps (100 × 100 μm²) of the S2p and C1s signals of the βCD SAM on Au^{TS} (the Ga_2O_3/EGaIn tip contacted the SAMs approximately in the middle of the image with a contact area of ~300 μm²). These XPS maps show no features (the bright band in the C1s signal is an artifact from the analyzer) and we conclude that the voltage pulses in our experiments did not significantly change the chemical composition of the supramolecular system on Au^{TS} during the experiments, or the nature of the Au^{TS}–molecule interface.

Dependence of R on the chemical structure of the electrodes: the top-electrode

Due to the liquid nature of the top-electrode material, we are not able to characterize the chemical composition of the Ga_2O_3/

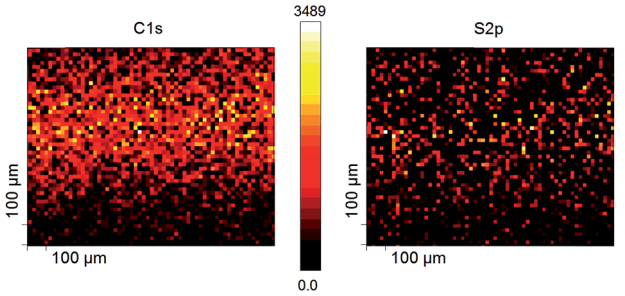

Fig. 4 XPS mapping plots of the Au^{TS}–βCDSAM//G1-PPI–$(Fc)_4$ surface of the elements C1s and S2p on an area that had been in contact with the top-electrode (the contact area of 300 μm^2 is approximately in the middle of the image of 100 × 100 μm^2), but the surrounding area not. See text for details.

EGaIn top-electrode after the $J(V)$ experiments as described above for the SAMs on Au^{TS}. Dickey and co-workers[77,78] reported the electrochemical anodic growth of the gallium oxide layer on the Ga_2O_3/EGaIn alloy and the cathodic dissolution of this gallium oxide layer in slightly acidic electrolyte solutions. To study the role of the thickness of the gallium oxide layer on the electrical characteristics of the junctions, we used two different methods to prepare intentionally oxidized Ga_2O_3/EGaIn cone-shaped tips. One method entailed electrochemical oxidation by once cycling the voltage between 0 and 1.0 V using water as the electrolyte and Pt as the counter electrode. The other method entailed oxidizing the Ga_2O_3/EGaIn tip suspended in air (with a relative humidity of 75%), using the same electrometer as was used to measure the electrical characteristics of the tunneling junctions, by simply applying a bias of 50 V to Ga_2O_3/EGaIn for 2 or 4 hours with a Au surface as the grounded counter electrode.

We measured the $J(V)$ characteristics of junctions of these intentionally oxidized Ga_2O_3/EGaIn electrodes in contact with Au^{TS}. Fig. 5A and B show the $J(V)$ curves obtained for a junction with oxidized Ga_2O_3/EGaIn top-electrodes in air for 4 hours and the histogram of the rectification ratios. These junctions rectified currents with $R = 4.5 \times 10^3$ determined at ±5.0 V.[84] Fig. S5† shows the results for junctions with a top-electrode with an electrochemically grown oxide layer with $R = 2.2 \times 10^2$ measured at ±1.5 V.[85] Unfortunately, the cone-shaped tips with native Ga_2O_3 did not form stable contacts with the metal surface and resulted in shorts. These results suggest that the oxidation of the Ga_2O_3/EGaIn electrode occurs at a lower applied bias and at smaller time scales in a wet electrochemical environment than under ambient conditions in air using an electrometer. Thus, we do not expect the formation of a thick layer of Ga_2O_3 in tunnel junctions with SAMs that do not contain chemisorbed water, or ions, at the experimental time scales and at applied voltages below the breakdown voltage.

We hypothesize that top-electrodes of Ga_2O_3/EGaIn that contains a thick layer of gallium oxides form non-ohmic contacts with the SAMs. To prove this hypothesis, we performed angle resolved XPS measurements on these oxidized Ga_2O_3/EGaIn surfaces prepared in air for 4 hours and on native Ga_2O_3/EGaIn surfaces. Fig. 5C and D show the XPS data before and after oxidation. We followed a previously reported method[21] to analyze the XPS data and derive the thickness of the Ga_2O_3 layer. Briefly, we determined from the relative intensities of Ga3d metal and oxide signals (Fig. 5C and D) and the corresponding Ga2p metal and oxide signals (see ESI, Fig. S6 and Table S1†) that we indeed form a thick layer of oxides of roughly 1.7 nm. We also estimated the increase of the thickness of the oxide layer during this experiment by ellipsometry and found that the oxide layer had a thickness of 2.3 nm (see ESI Fig. S8 and Table S2†). From these experiments, we conclude that the oxide layer in the tunneling junctions likely increased its thickness from 0.7 nm to roughly 2 nm (see ESI Fig. S8 and Table S2†).

To compare the electronic surface properties of the native and the oxidized Ga_2O_3/EGaIn we measured ultra-violet photoelectron spectra (UPS) on drops of Ga_2O_3/EGaIn before and after oxidation in air, with the zero energy normalized to the Fermi level of clean Au. From the UPS measurements it can be seen that the work function (ϕ) of the oxidized Ga_2O_3/EGaIn (ϕ = 3.70 eV) is 0.1 eV higher than that for native Ga_2O_3/EGaIn (ϕ = 3.60 eV; Fig. 5E), and likewise, the valence band maximum energies (VBM) for the oxidized Ga_2O_3/EGaIn (4.15 eV) is 0.3 eV higher than for native Ga_2O_3/EGaIn (3.85 eV; Fig. 5F). Therefore, the valance band (ϕ + VBM) of the native and oxidized Ga_2O_3/EGaIn was determined to be 7.45 eV and 7.85 eV, respectively, with respect to the vacuum level. Bulk Ga_2O_3 fabricated under normal conditions, that is, not under highly controlled conditions to avoid defects, is an n-type transparent semiconductor with a band gap of about 4.8 eV.[86–88] Considering this band gap, the conduction band of the native and oxidized Ga_2O_3/EGaIn is only 0.95 eV and 0.65 eV, respectively, above the Fermi level. This implies that in both cases the Ga_2O_3 layer is an n-type semiconductor, with the oxidized Ga_2O_3/EGaIn sample being a higher doped n-type conductor than the native Ga_2O_3/EGaIn sample. Therefore, the UPS data are consistent with the oxidized Ga_2O_3/EGaIn sample having a thicker Ga_2O_3 layer, as the oxidized Ga_2O_3/EGaIn sample is shown to be a higher doped n-type conductor and has a higher work function, VBM and thus valance band energy. This means that more energy is needed to eject an electron from the Fermi level/move an electron from the valance band to the conduction band of EGaIn. We note that the energy levels determined for the Ga_2O_3/EGaIn surfaces will shift once these surfaces are incorporated into a junction.[6,89,90] We expect these shifts to be small as the GaO_x/EGaIn forms a van der Waals contact with most types of monolayers[59,69,91] and therefore our UPS measurements provide reasonable description of the energy levels.

We believe that the oxidized Ga_2O_3 layer, with ϕ = 3.70 eV, in contact with the Au bottom electrode, with ϕ = 4.8 eV, will be positively charged because of the imbalance of the work function between Au and Ga_2O_3/EGaIn. From Kelvin probe measurements on Ga_2O_3/EGaIn, we obtained the work function (ϕ) of the bulk EGaIn of 4.3 eV. This so-called "space charge" phenomenon could result in a non-ohmic contact between the oxidized Ga_2O_3/EGaIn electrode and the Au, and the large observed rectification ratio of 4.5×10^3 (Fig. 5A and B).

Thus, we believe that during our $J(V)$ measurements of junctions of supramolecular assemblies, the native Ga_2O_3/

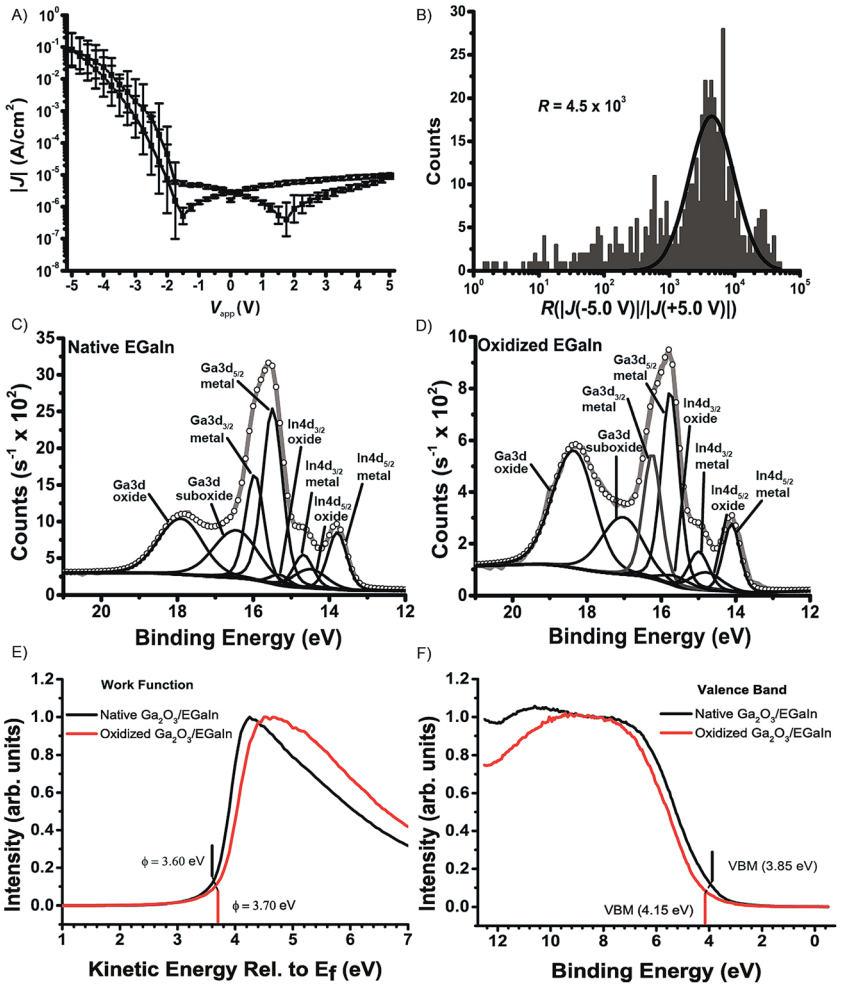

Fig. 5 (A) Semi-log plot of averaged $|J|$ *vs.* (V) measurements performed at ±5.0 V on junctions of Au^{TS}//Ga_2O_3/EGaIn. (B) Histogram of log rectification ratio (R), where $R = |J|(-5.0\ V)/|J|(+5.0\ V)$. Note that R is only defined at ±5.0 V for the junction Au^{TS}//Ga_2O_3/EGaIn. (C and D) High resolution XPS spectrum of the Ga3d/In4d region for native (C) and oxidized (D) Ga_2O_3/EGaIn samples. (E and F) UPS spectra for native and oxidized Ga_2O_3/EGaIn samples, showing the difference in work function (E) and valence band (F) energies.

EGaIn reacts with water and ions present in the junctions and forms a thick layer of gallium oxide when the tip is positively biased. This *in situ* formed layer of gallium oxide of ~2 nm on the top Ga_2O_3/EGaIn electrode causes the top electrode to form a non-ohmic contact with the SAM resulting in values of R exceeding four orders of magnitude. This hypothesis agrees with our observations: (i) a large increase in the value of R is only observed when positive biases, and not when negative biases, are applied to the top-electrode which agrees with electrochemical measurements which show that the thickness of Ga_2O_3 only increases at a positive bias and (ii) the $J(V)$ characteristics of the junctions with thick layers of Ga_2O_3 are independent of the chemical composition of the supramolecular junctions as expected for junctions dominated by a non-ohmic contact (Fig. 3A).

Conclusions

Stable supramolecular tunneling junctions were formed with a top Ga_2O_3/EGaIn cone shaped electrode suspended from a syringe in contact with a monolayer of dendrimers adsorbed on a well-defined hexagonally packed heptathioether βCD SAM on Au^{TS}. The junctions were stable over periods of time of more than 16 h and could sustain applied voltages of up to +2.5 V. The rectification ratio R of the supramolecular tunneling junctions increased by three to four orders of magnitude when the top-electrode was biased at +2.5 V for 3600 s. The change in the value of R during these experiments is independent of the supramolecular and chemical structure of the SAMs inside the junctions, but depends on the applied bias to the Ga_2O_3/EGaIn top-electrode and the duration of this voltage pulse.

The observed increase in the rectification ratio originates from changes in the chemical composition of the Ga_2O_3/EGaIn top-electrode, where the thickness of the gallium oxide layer, that was initially only 0.7 nm thick, increased to ~2 nm when the top-electrode was positively biased, due to the presence of chemisorbed water and ions, *i.e.*, H_3O^+, protonated amines with predominantly Cl^- counter ions, in the supramolecular SAM. This in turn changes the originally ohmic SAM//Ga_2O_3/EGaIn contact to a non-ohmic contact. This hypothesis was supported

by the following experiments. (i) The rectifying supramolecular junctions were disassembled to investigate the chemical properties by XPS before and after the SAMs had been subjected to a voltage pulse of +2.5 V for 900 s. The XPS data recorded on both types of SAMs were indistinguishable, which meant that neither the SAMs nor the Au–molecule interface changed their chemical composition. (ii) A thick Ga_2O_3 layer was formed on a tip of Ga_2O_3/EGaIn. Junctions of these tips in contact with bare gold surfaces rectified currents with values of $R \approx 10^2$ to 10^3. (iii) Ellipsometry and XPS measurements were performed on samples of intentionally oxidized Ga_2O_3/EGaIn and were compared to native Ga_2O_3/EGaIn samples. Each characterization technique showed that the oxidized Ga_2O_3/EGaIn had a thicker Ga_2O_3 layer (~2 nm) than the native Ga_2O_3/EGaIn (0.7 nm).

One of the major goals in molecular electronics is to disentangle the molecular contributions to the electronic characteristics from non-molecular contributions induced by the interfaces, electrode materials, and, in this case, the presence of metal oxides. The difficulty in doing so is that every molecular electronic device is a complex physical-organic system whose properties depends on all elements, including the organic/molecular parts, electrodes, and interfaces. Previous studies involving SAM-based junctions with Ga_2O_3/EGaIn top-electrodes using SAMs of the form of $SC_{n-1}CH_3$, SC_nFc, conjugated thiols, and *n*-alkanethiolates with various end groups, have been all conducted in the bias regime of ±1.0 V (because of the electric break down at higher biases resulting in shorts). In this low bias regime of ±1.0 V, the growth of the gallium oxide layer is very slow and time dependent changes in the electrical characterization of these junctions were not observed. In contrast, this study involved junctions with supramolecular SAMs that contain chemisorbed water and ions, in the high bias regime of >±1.0 V, the growth of the gallium oxide layer was significant resulting in an exponential increase of the rectification ratio as a function of bias (Fig. S2F†). Currently, we do not know the kinetics of the growth of the Ga_2O_3 layer in our experimental conditions, but the maximum values of *R* for a V_{pulse} at a given voltage are reached in about 1800 seconds and increase with increasing value of V_{pulse}. Thus, we conclude that the electrical characteristics of junctions measured with the "EGaIn-technique" are dominated by the molecular properties of the junctions for biases <±1.0 V and that experiments involving large bias ranges should be performed with care and include appropriate control experiments.

We conclude that a thin Ga_2O_3 layer of 0.7 nm allows the top Ga_2O_3/EGaIn electrode to form an ohmic contact with the SAM because as all studies involving SAMs in contact with Ga_2O_3/EGaIn top-electrodes did not change their electrical characteristics as a function of voltage cycling at a range of applied voltages of ±1.0 V, and did show statistically significant molecular effects which would not be expected in the case of non-ohmic contacts. In other words, the values of *R* in all of these studies were not influenced by the native layer of Ga_2O_3. Additionally, we conclude that a thick layer of Ga_2O_3 on the Ga_2O_3/EGaIn electrode of ~2 nm is thick enough to form a non-ohmic contact as junctions that contain chemisorbed water and ions did change their electrical characteristics as a function of the number of voltage cycles when biases ≥+2.0 were involved, and did not reveal molecular effects on the electrical characteristics of the junctions when voltage pulses of +2.5 V (stepped from 0 V to 2.5 and stepped back to 0 V after a predefined time interval) were applied.

The presence of layers of metal-oxides in top contacts such as Al_2O_3/Al and TiO_2/Ti has been shown to be the source of rectification in molecular tunneling junctions in other systems.[30,32,36,79] In all studies thus far involving the EGaIn-technique in the bias regime of <±1.0 V, no direct evidence was found that the Ga_2O_3 layer dominated the charge transport properties. For these reasons, the "EGaIn" technique is a very reliable technique to study charge transport across SAMs in the bias regime of ±1.0 V, and the gallium oxide layer does not dominate the mechanisms of charge transport. In one of our previous studies *J*(*V*) measurements were performed in a bias range of ±2.0 V on SAMs that did contain chemisorbed water and a source of H_3O^+.[67] However, that study did not involve more than 20 *J*(*V*) scans on a single junction and therefore, it is safe to conclude that the *J*(*V*) characteristics were dominated by the molecular structure within the junction.[67] Our results discussed here demonstrate that studies involving large applied biases, and/or structures that contain chemisorbed water can be performed, but with constraints as anodic growth of gallium oxides may occur when large bias windows are used.

Acknowledgements

The Singapore National Research Foundation (NRF Award no. NRF-RF2010-03 to C.A.N.) is kindly acknowledged for supporting this research. We gratefully thank Dr Anton V. Sadovoy (Institute of Materials Research and Engineering) for the very useful discussions and suggestions, Zhang Zheng (Institute of Material Research and Engineering) for performing the XPS and UPS measurements on the native and oxidized Ga_2O_3/EGaIn films, Zheng Yi (National University of Singapore) for performing the Kelvin Probe measurements on EGaIn and Gerard Kip (MESA$^+$ Institute for Nanotechnology at the University of Twente) for performing the XPS surface mapping experiments.

References

1 M. Grätzel, R. A. J. Janssen, D. B. Mitzi and E. H. Sargent, Materials Interface Engineering for Solution-Processed Photovoltaics, *Nature*, 2012, **488**, 304–312.
2 M. P. de Jong, L. J. van Ijzendoorn and M. J. A. de Voigt, Stability of the Interface Between Indium-Tin-Oxide and Poly(3,4-ethylenedioxythiophene)/Poly(styrenesulfonate) in Polymer Light-Emitting Diodes, *Appl. Phys. Lett.*, 2000, **77**, 2255–2257.
3 S. Wang, P. K. Ang, Z. Wang, A. L. L. Tang, J. T. L. Thong and K. P. Loh, High Mobility, Printable, and Solution-Processed Graphene Electronics, *Nano Lett.*, 2010, **10**, 92–98.
4 A. Nitzan, Electron Transmission Through Molecules and Molecular Interfaces, *Annu. Rev. Phys. Chem.*, 2001, **52**, 681–750.

5 D. M. Adams, L. Brus, C. E. D. Chidsey, S. Creager, C. Creutz, C. R. Kagan, P. V. Kamat, M. Lieberman, S. Lindsay, R. A. Marcus, R. M. Metzger, M. E. Michel-Beyerle, J. R. Miller, M. D. Newton, D. R. Rolison, O. Sankey, K. S. Schanze, J. Yardley and X. Y. Zhu, Charge Transfer on the Nanoscale: Current Status, *J. Phys. Chem. B*, 2003, **107**, 6668–6697.

6 N. Koch, Organic Electronic Devices and Their Functional Interfaces, *ChemPhysChem*, 2007, **8**, 1438–1455.

7 P. K. H. Ho, J. S. Kim, J. H. Burroughes, H. Becker, S. F. Y. Li, T. M. Brown, F. Cacialli and R. H. Friend, Molecular-Scale Interface Engineering for Polymer Light-Emitting Diodes, *Nature*, 2000, **404**, 481–484.

8 C.-A. Di, Y. Liu, G. Yu and D. Zhu, Interface Engineering: An Effective Approach toward High-Performance Organic Field-Effect Transistors, *Acc. Chem. Res.*, 2009, **42**, 1573–1583.

9 H. Ishii, K. Sugiyama, E. Ito and K. Seki, Energy Level Alignment and Interfacial Electronic Structures at Organic Metal and Organic Organic Interfaces, *Adv. Mater.*, 1999, **11**, 605–625.

10 G. Heimel, L. Romaner, E. Zojer and J.-L. Bredas, The Interface Energetics of Self-Assembled Monolayers on Metals, *Acc. Chem. Res.*, 2008, **41**, 721–729.

11 M. T. Greiner, M. G. Helander, W.-M. Tang, Z.-B. Wang, J. Qiu and Z.-H. Lu, Universal Energy-Level Alignment of Molecules on Metal Oxides, *Nat. Mater.*, 2012, **11**, 76–81.

12 J. M. Seminario, C. E. De la Cruz and P. A. Derosa, A Theoretical Analysis of Metal–Molecule Contacts, *J. Am. Chem. Soc.*, 2001, **123**, 5616–5617.

13 K. W. Hipps, Molecular Electronics – It's All About Contacts, *Science*, 2001, **294**, 536–537.

14 B. Kim, S. H. Choi, X. Y. Zhu and C. D. Frisbie, Molecular Tunnel Junctions Based on pi-Conjugated Oligoacene Thiols and Dithiols between Ag, Au, and Pt Contacts: Effect of Surface Linking Group and Metal Work Function, *J. Am. Chem. Soc.*, 2011, **133**, 19864–19877.

15 G. Ricoeur, S. Lenfant, D. Guerin and D. Vuillaume, Molecule/Electrode Interface Energetics in Molecular Junction: A "Transition Voltage Spectroscopy" Study, *J. Phys. Chem. C*, 2012, **116**, 20722–20730.

16 V. V. Zhirnov and R. K. Cavin, Molecular Electronics: Chemistry of Molecules or Physics of Contacts?, *Nat. Mater.*, 2006, **5**, 11–12.

17 W. Hong, D. Z. Manrique, P. Moreno-García, M. Gulcur, A. Mishchenko, C. J. Lambert, M. R. Bryce and T. Wandlowski, Single Molecular Conductance of Tolanes: Experimental and Theoretical Study on the Junction Evolution Dependent on the Anchoring Group, *J. Am. Chem. Soc.*, 2011, **134**, 2292–2304.

18 X. D. Cui, X. Zarate, J. Tomfohr, O. F. Sankey, A. Primak, A. L. Moore, T. A. Moore, D. Gust, G. Harris and S. M. Lindsay, Making Electrical Contacts to Molecular Monolayers, *Nanotechnology*, 2002, **13**, 5–14.

19 F. Chen, X. Li, J. Hihath, Z. Huang and N. Tao, Effect of Anchoring Groups on Single-Molecule Conductance: Comparative Study of Thiol-, Amine-, and Carboxylic-Acid-Terminated Molecules, *J. Am. Chem. Soc.*, 2006, **128**, 15874–15881.

20 Y. S. Park, A. C. Whalley, M. Kamenetska, M. L. Steigerwald, M. S. Hybertsen, C. Nuckolls and L. Venkataraman, Contact Chemistry and Single-Molecule Conductance: A Comparison of Phosphines, Methyl Sulfides, and Amines, *J. Am. Chem. Soc.*, 2007, **129**, 15768–15769.

21 L. Cademartiri, M. M. Thuo, C. A. Nijhuis, W. F. Reus, S. Tricard, J. R. Barber, R. N. S. Sodhi, P. Brodersen, C. Kim, R. C. Chiechi and G. M. Whitesides, Electrical Resistance of Ag^{TS}–$S(CH_2)_{n-1}CH_3$//Ga_2O_3/EGaln Tunneling Junctions, *J. Phys. Chem. C*, 2012, **116**, 10848–10860.

22 W. F. Reus, M. M. Thuo, N. D. Shapiro, C. A. Nijhuis and G. M. Whitesides, The SAM, Not the Electrodes, Dominates Charge Transport in Metal-Monolayer//Ga_2O_3/Gallium-Indium Eutectic Junctions, *ACS Nano*, 2012, **6**, 4806–4822.

23 A. J. Kronemeijer, I. Katsouras, E. H. Huisman, P. A. van Hal, T. C. T. Geuns, P. W. M. Blom and D. M. de Leeuw, Universal Scaling of the Charge Transport in Large-Area Molecular Junctions, *Small*, 2011, **7**, 1593–1598.

24 G. Wang, T. W. Kim, H. Lee and T. Lee, Influence of Metal–Molecule Contacts on Decay Coefficients and Specific Contact Resistances in Molecular Junctions, *Phys. Rev. B: Condens. Matter Mater. Phys.*, 2007, **76**, 205320.

25 H. Haick and D. Cahen, Making Contact: Connecting Molecules Electrically to the Macroscopic World, *Prog. Surf. Sci.*, 2008, **83**, 217–261.

26 A. Danilov, S. Kubatkin, S. Kafanov, P. Hedegard, N. Stuhr-Hansen, K. Moth-Poulsen and T. Bjornholm, Electronic Transport in Single Molecule Junctions: Control of the Molecule–Electrode Coupling Through Intramolecular Tunneling Barriers, *Nano Lett.*, 2008, **8**, 1–5.

27 S. M. Lindsay and M. A. Ratner, Molecular Transport Junctions: Clearing Mists, *Adv. Mater.*, 2007, **19**, 23–31.

28 H. B. Akkerman and B. de Boer, Electrical Conduction Through Single Molecules and Self-Assembled Monolayers, *J. Phys.: Condens. Matter*, 2008, **20**, 013001.

29 D. A. Bell, *Fundamentals of Electronic Devices and Circuits*, Oxford University Press, Incorporated, 2008.

30 R. McCreery, J. Dieringer, A. O. Solak, B. Snyder, A. M. Nowak, W. R. McGovern and S. DuVall, Molecular Rectification and Conductance Switching in Carbon-Based Molecular Junctions by Structural Rearrangement Accompanying Electron Injection, *J. Am. Chem. Soc.*, 2003, **125**, 10748–10758.

31 A. J. Bergren, K. D. Harris, F. Deng and R. McCreery, Molecular Electronics Using Diazonium-Derived Adlayers on Carbon with Cu Top Contacts: Critical Analysis of Metal Oxides and Filaments, *J. Phys.: Condens. Matter*, 2008, **20**, 374117.

32 H.-J. Che, P.-J. Chia, L.-L. Chua, S. Sivaramakrishnan, J.-C. Tang, A. T. S. Wee, H. S. O. Chan and P. K. H. Ho, Robust Reproducible Large-Area Molecular Rectifier Junctions, *Appl. Phys. Lett.*, 2008, **92**, 253503.

33 N. J. Geddes, J. R. Sambles, D. J. Jarvis, W. G. Parker and D. J. Sandman, The Electrical-Properties of Metal-Sandwiched Langmuir–Blodgett Multilayers and

Monolayers of a Redox-Active Organic Molecular-Compound, *J. Appl. Phys.*, 1992, **71**, 756–768.

34 C. A. Nijhuis, W. F. Reus and G. M. Whitesides, Molecular Rectification in Metal–SAM–Metal Oxide–Metal Junctions, *J. Am. Chem. Soc.*, 2009, **131**, 17814–17827.

35 C. A. Nijhuis, W. F. Reus, J. R. Barber, M. D. Dickey and G. M. Whitesides, Charge Transport and Rectification in Arrays of SAM-Based Tunneling Junctions, *Nano Lett.*, 2010, **10**, 3611–3619.

36 R. M. Metzger, Electrical Rectification by a Molecule: The Advent of Unimolecular Electronic Devices, *Acc. Chem. Res.*, 1999, **32**, 950–957.

37 N. Nerngchamnong, L. Yuan, D.-C. Qi, J. Li, D. Thompson and C. A. Nijhuis, The Role of van der Waals Forces in the Performance of Molecular Diodes, *Nat. Nanotechnol.*, 2013, **8**, 113–118.

38 V. Mujica, M. A. Ratner and A. Nitzan, Molecular Rectification: Why Is it So Rare?, *Chem. Phys.*, 2002, **281**, 147–150.

39 R. L. McCreery and A. J. Bergren, Progress with Molecular Electronic Junctions: Meeting Experimental Challenges in Design and Fabrication, *Adv. Mater.*, 2009, **21**, 4303–4322.

40 J. Cornil, D. Beljonne, J. P. Calbert and J. L. Bredas, Interchain Interactions in Organic pi-Conjugated Materials: Impact on Electronic Structure, Optical Response, and Charge Transport, *Adv. Mater.*, 2001, **13**, 1053–1067.

41 K. Moth-Poulsen and T. Bjornholm, Molecular Electronics with Single Molecules in Solid-State Devices, *Nat. Nanotechnol.*, 2009, **4**, 551–556.

42 C. N. Lau, D. R. Stewart, R. S. Williams and M. Bockrath, Direct Observation of Nanoscale Switching Centers in Metal/Molecule/Metal Structures, *Nano Lett.*, 2004, **4**, 569–572.

43 J. M. Beebe and J. G. Kushmerick, Nanoscale Switch Elements from Self-Assembled Monolayers on Silver, *Appl. Phys. Lett.*, 2007, **90**, 083117.

44 G. L. Fisher, A. V. Walker, A. E. Hooper, T. B. Tighe, K. B. Bahnck, H. T. Skriba, M. D. Reinard, B. C. Haynie, R. L. Opila, N. Winograd and D. L. Allara, Bond Insertion, Complexation, and Penetration Pathways of Vapor-Deposited Aluminum Atoms with HO- and CH_3O-Terminated Organic Monolayers, *J. Am. Chem. Soc.*, 2002, **124**, 5528–5541.

45 A. V. Walker, T. B. Tighe, O. M. Cabarcos, M. D. Reinard, B. C. Haynie, S. Uppili, N. Winograd and D. L. Allara, The Dynamics of Noble Metal Atom Penetration Through Methoxy-Terminated Alkanethiolate Monolayers, *J. Am. Chem. Soc.*, 2004, **126**, 3954–3963.

46 G. S. Bang, H. Chang, J. R. Koo, T. Lee, R. C. Advincula and H. Lee, High-Fidelity Formation of a Molecular-Junction Device Using a Thickness-Controlled Bilayer Architecture, *Small*, 2008, **4**, 1399–1405.

47 T.-W. Kim, G. Wang, H. Lee and T. Lee, Statistical Analysis of Electronic Properties of Alkanethiols in Metal–Molecule–Metal Junctions, *Nanotechnology*, 2007, **18**, 315204.

48 J. Deng, W. Hofbauer, N. Chandrasekhar and S. J. O'Shea, Metallization for Crossbar Molecular Devices, *Nanotechnology*, 2007, **18**, 155202.

49 A. Salomon, T. Boecking, O. Seitz, T. Markus, F. Amy, C. Chan, W. Zhao, D. Cahen and A. Kahn, What is the Barrier for Tunneling Through Alkyl Monolayers? Results from n- and p-Si-Alkyl/Hg Junctions, *Adv. Mater.*, 2007, **19**, 445–450.

50 R. E. Holmlin, R. Haag, M. L. Chabinyc, R. F. Ismagilov, A. E. Cohen, A. Terfort, M. A. Rampi and G. M. Whitesides, Electron Transport through Thin Organic Films in Metal–Insulator–Metal Junctions Based on Self-Assembled Monolayers, *J. Am. Chem. Soc.*, 2001, **123**, 5075–5085.

51 F. Milani, C. Grave, V. Ferri, P. Samori and M. A. Rampi, Ultrathin pi-Conjugated Polymer Films for Simple Fabrication of Large-Area Molecular Junctions, *ChemPhysChem*, 2007, **8**, 515–518.

52 R. L. York, P. T. Nguyen and K. Slowinski, Long-Range Electron Transfer through Monolayers and Bilayers of Alkanethiols in Electrochemically Controlled Hg–Hg tunneling junctions, *J. Am. Chem. Soc.*, 2003, **125**, 5948–5953.

53 G. Wang, Y. Kim, M. Choe, T. W. Kim and T. Lee, A New Approach for Molecular Electronic Junctions with a Multilayer Graphene Electrode, *Adv. Mater.*, 2011, **23**, 755–760.

54 T. Li, J. R. Hauptmann, Z. Wei, S. Petersen, N. Bovet, T. Vosch, J. Nygard, W. Hu, Y. Liu, T. Bjornholm, K. Norgaard and B. W. Laursen, Solution-Processed Ultrathin Chemically Derived Graphene Films as Soft Top Contacts for Solid-State Molecular Electronic Junctions, *Adv. Mater.*, 2012, **24**, 1333–1339.

55 S. Seo, M. Min, J. Lee, T. Lee, S.-Y. Choi and H. Lee, Solution-Processed Reduced Graphene Oxide Films as Electronic Contacts for Molecular Monolayer Junctions, *Angew. Chem., Int. Ed.*, 2012, **51**, 108–112.

56 S. Park, G. Wang, B. Cho, Y. Kim, S. Song, Y. Ji, M.-H. Yoon and T. Lee, Flexible Molecular-Scale Electronic Devices, *Nat. Nanotechnol.*, 2012, **7**, 438–442.

57 G. Wang, S.-I. Na, T.-W. Kim, Y. Kim, S. Park and T. Lee, Effect of PEDOT:PSS-Molecule Interface on the Charge Transport Characteristics of the Large-Area Molecular Electronic Junctions, *Org. Electron.*, 2012, **13**, 771–777.

58 R. C. Chiechi, E. A. Weiss, M. D. Dickey and G. M. Whitesides, Eutectic Gallium-Indium (EGaIn): A Moldable Liquid Metal for Electrical Characterization of Self-Assembled Monolayers, *Angew. Chem., Int. Ed.*, 2008, **47**, 142–144.

59 H. J. Yoon, N. D. Shapiro, K. M. Park, M. M. Thuo, S. Soh and G. M. Whitesides, The Rate of Charge Tunneling through Self-Assembled Monolayers Is Insensitive to Many Functional Group Substitutions, *Angew. Chem., Int. Ed.*, 2012, **51**, 4658–4661.

60 W. F. Reus, C. A. Nijhuis, J. R. Barber, M. M. Thuo, S. Tricard and G. M. Whitesides, Statistical Tools for Analyzing Measurements of Charge Transport, *J. Phys. Chem. C*, 2012, **116**, 6714–6733.

61 D. Fracasso, H. Valkenier, J. C. Hummelen, G. C. Solomon and R. C. Chiechi, Evidence for Quantum Interference in SAMs of Arylethynylene Thiolates in Tunneling Junctions with Eutectic Ga-In (EGaIn) Top-Contacts, *J. Am. Chem. Soc.*, 2011, **133**, 9556–9563.

62 D. Fracasso, M. I. Muglali, M. Rohwerder, A. Terfort and R. C. Chiechi, Influence of an Atom in EGaIn/Ga_2O_3 Tunneling Junctions Comprising Self-Assembled Monolayers, *J. Phys. Chem. C*, 2013, **117**, 11367–11376.

63 M. M. Thuo, W. F. Reus, C. A. Nijhuis, J. R. Barber, C. Kim, M. D. Schulz and G. M. Whitesides, Odd–Even Effects in Charge Transport across Self-Assembled Monolayers, *J. Am. Chem. Soc.*, 2011, **133**, 2962–2975.

64 C. A. Nijhuis, W. F. Reus and G. M. Whitesides, Mechanism of Rectification in Tunneling Junctions Based on Molecules with Asymmetric Potential Drops, *J. Am. Chem. Soc.*, 2010, **132**, 18386–18401.

65 C. A. Nijhuis, W. F. Reus, A. C. Siegel and G. M. Whitesides, A Molecular Half-Wave Rectifier, *J. Am. Chem.Soc.*, 2011, **133**, 15397–15411.

66 C. A. Nijhuis, W. F. Reus, J. R. Barber and G. M. Whitesides, Comparison of SAM-Based Junctions with Ga_2O_3/EGaln Top Electrodes to Other Large-Area Tunneling Junctions, *J. Phys. Chem. C*, 2012, **116**, 14139–14150.

67 K. S. Wimbush, W. F. Reus, W. G. van der Wiel, D. N. Reinhoudt, G. M. Whitesides, C. A. Nijhuis and A. H. Velders, Control over Rectification in Supramolecular Tunneling Junctions, *Angew. Chem., Int. Ed.*, 2010, **49**, 10176–10180.

68 A. M. Masillamani, N. Crivillers, E. Orgiu, J. Rotzler, D. Bossert, R. Thippeswamy, M. Zharnikov, M. Mayor and P. Samori, Multiscale Charge Injection and Transport Properties in Self-Assembled Monolayers of Biphenyl Thiols with Varying Torsion Angles, *Chem.–Eur. J.*, 2012, **18**, 10335–10347.

69 H. J. Yoon, C. M. Bowers, M. Baghbanzadeh and G. M. Whitesides, The Rate of Charge Tunneling Is Insensitive to Polar Terminal Groups in Self-Assembled Monolayers in (AgS)-S-TS$(CH_2)(n)$M$(CH_2)(m)$T//Ga_2O_3/EGaIn Junctions, *J. Am. Chem. Soc.*, 2014, **136**, 16–19.

70 F. C. Simeone, H. J. Yoon, M. M. Thuo, J. R. Barber, B. Smith and G. M. Whitesides, Defining the Value of Injection Current and Effective Electrical Contact Area for EGaIn-Based Molecular Tunneling Junctions, *J. Am. Chem. Soc.*, 2013, **135**, 18131–18144.

71 M. J. Regan, H. Tostmann, P. S. Pershan, O. M. Magnussen, E. DiMasi, B. M. Ocko and M. Deutsch, X-Ray Study of the Oxidation of Liquid-Gallium Surfaces, *Phys. Rev. B: Condens. Matter Mater. Phys.*, 1997, **55**, 10786–10790.

72 M. W. J. Beulen, J. Bügler, M. R. de Jong, B. Lammerink, J. Huskens, H. Schönherr, G. J. Vancso, B. A. Boukamp, H. Wieder, A. Offenhäuser, W. Knol, F. C. J. M. van Veggel and D. N. Reinhoudt, Host–Guest Interactions at Self-Assembled Monolayers of Cyclodextrins on Gold, *Chem.–Eur. J.*, 2000, **6**, 1176–1183.

73 M. W. J. Beulen, J. Bugler, B. Lammerink, F. A. J. Geurts, E. M. E. F. Biemond, K. G. C. van Leerdam, F. C. J. M. van Veggel, J. F. J. Engbersen and D. N. Reinhoudt, Self-Assembled Monolayers of Heptapodant β-Cyclodextrins on Gold, *Langmuir*, 1998, **14**, 6424–6429.

74 J. Huskens, M. A. Deij and D. N. Reinhoudt, Attachment of Molecules at a Molecular Printboard by Multiple Host–Guest Interactions, *Angew. Chem., Int. Ed.*, 2002, **41**, 4467–4471.

75 C. A. Nijhuis, J. Huskens and D. N. Reinhoudt, Binding Control and Stoichiometry of Ferrocenyl Dendrimers at a Molecular Printboard, *J. Am. Chem. Soc.*, 2004, **126**, 12266–12267.

76 C. A. Nijhuis, F. Yu, W. Knoll, J. Huskens and D. N. Reinhoudt, Multivalent Dendrimers at Molecular Printboards: Influence of Dendrimer Structure on Binding Strength and Stoichiometry and Their Electrochemically Induced Desorption, *Langmuir*, 2005, **21**, 7866–7876.

77 J. H. So, H. J. Koo, M. D. Dickey and O. D. Velev, Ionic Current Rectification in Soft-Matter Diodes with Liquid-Metal Electrodes, *Adv. Funct. Mater.*, 2012, **22**, 625–631.

78 H.-J. Koo, J.-H. So, M. D. Dickey and O. D. Velev, Towards All-Soft Matter Circuits: Prototypes of Quasi-Liquid Devices with Memristor Characteristics, *Adv. Mater.*, 2011, **23**, 3559–3564.

79 R. McCreery, J. Dieringer, A. O. Solak, B. Snyder, A. M. Nowak, W. R. McGovern and S. DuVall, Molecular Rectification and Conductance Switching in Carbon-Based Molecular Junctions by Structural Rearrangement Accompanying Electron Injection (2003, **125**, 10748), *J. Am. Chem. Soc.*, 2004, **126**, 6200.

80 R. Haag, M. A. Rampi, R. E. Holmlin and G. M. Whitesides, Electrical Breakdown of Aliphatic and Aromatic Self-Assembled Monolayers Used as Nanometer-Thick Organic Dielectrics, *J. Am. Chem. Soc.*, 1999, **121**, 7895–7906.

81 I. Cuadrado, M. Moran, C. M. Casado, B. Alonso, F. Lobete, B. Garcia, M. Ibisate and J. Losada, Ferrocenyl-Functionalized Poly(propylenimine) Dendrimers, *Organometallics*, 1996, **15**, 5278–5280.

82 J. Huskens, A. Mulder, T. Auletta, C. A. Nijhuis, M. J. W. Ludden and D. N. Reinhoudt, A Model for Describing the Thermodynamics of Multivalent Host–Guest Interactions at Interfaces, *J. Am. Chem. Soc.*, 2004, **126**, 6784–6797.

83 A. Mulder, T. Auletta, A. Sartori, S. Del Ciotto, A. Casnati, R. Ungaro, J. Huskens and D. N. Reinhoudt, Divalent Binding of a Bis(adamantyl)-Functionalized Calix[4]arene to β-Cyclodextrin-Based Hosts: An Experimental and Theoretical Study on Multivalent Binding in Solution and at Self-Assembled Monolayers, *J. Am. Chem. Soc.*, 2004, **126**, 6627–6636.

84 The value of R was determined at ± 5.0 V because the thick oxide layer does not form good conformal contact with the Au^{TS} surface which causes a large contact resistance.

85 For these junctions R was determined at ± 1.5 V as these junctions repeatedly shorted at a bias of ± 2.0 V.

86 M. Fleischer and H. Meixner, Electron-Mobility in Single-Crystalline and Polycrystalline Ga_2O_3, *J. Appl. Phys.*, 1993, **74**, 300–305.

87 M. R. Lorenz, J. F. Woods and R. J. Gambino, Some Electrical Properties of Semiconductor of β-Ga_2O_3, *J. Phys. Chem. Solids*, 1967, **28**, 403–404.

88 H. Hosono, Recent progress in transparent oxide semiconductors: Materials and device application, *Thin Solid Films*, 2007, **515**, 6000–6014.

89 I. Bâldea, A quantum chemical study from a molecular perspective: ionization and electron attachment energies for species often used to fabricate single-molecule junctions, *Faraday Discuss.*, 2014, DOI: 10.1039/c4fd00101j.

90 O. Yaffe, Y. Qi, L. Sheres, S. R. Puniredd, L. Segev, T. Ely, H. Haick, H. Zuilhof, A. Vilan, L. Kronik, A. Kahn and D. Cahen, Charge transport across metal/molecular (alkyl) monolayer-Si junctions is dominated by the LUMO level, *Phys. Rev. B: Condens. Matter Mater. Phys.*, 2012, **85**, 045433.

91 C. M. Bowers, K.-C. Liao, J. Y. Yoon, D. Rappoport, M. Baghbanzadeh, F. C. Simeone and G. M. Whitesides, Introducing Ionic and/or Hydrogen Bonds into the SAM//Ga_2O_3 Top-Interface of $Ag^{TS}/S(CH_2)_nT//Ga_2O_3$/EGaIn Junctions, *Nano Lett.*, 2014, **14**, 3521–3526.